

Specificity of Mono- and Disilane Decomposition at Silicon Surface under Conditions of Epitaxial Growth

L. K. Orlov^{a,b}, N. L. Ivina^{a,c}, and T. N. Smyslova^a

^a Alekseev Nizhni Novgorod State Technical University, ul. Minina 24, Nizhni Novgorod, 603950 Russia
e-mail: orlov@ipm.sci-nnov.ru

^b Institute for Physics of Microstructures, Russian Academy of Sciences, Nizhni Novgorod, Russia

^c Nizhni Novgorod Institute of Management, Nizhni Novgorod, Russia

Received November 8, 2012

Abstract—Basic kinetic parameters of surface hydrogen desorption and of adsorbed silicon hydrides decomposition has been evaluated by kinetic simulation based on data of the technological experiments on silicon layer growth at 450–700°C. For the molecular epitaxial growth, the silicon surface population with silicon hydrides fragments has been estimated. The relationship between the surface hydrides pyrolysis frequency and the rate of silicon atoms incorporation into the growing crystal has been found.

DOI: 10.1134/S1070363213120037

The interaction of molecular beam with the solid surface and the related interface phenomena underlie many practically important technological processes. The most important of them are catalysis, membrane gas separation, homoepitaxy, and heteroepitaxy. Recently, monoatomic and monomolecular films like monoatomic grapheme layers and monomolecular Langmuir-Blodgett films at the liquid interface has attracted a great deal of attention. Therefore, the methods of monomolecular layers preparation on the solid surface have been intensively developed, the most widely spread being molecular layering and layer buildup in a vacuum using molecular sources.

The controlled preparation of monoatomic surface heterocompositions is of extreme importance in the fields of nanotechnology and nanoelectronics. The vacuum chemical epitaxy method is commonly used to form perfect thin film compositions and two-dimensional surface structures. The layers are usually grown at relatively high temperature under conditions when the surface is covered with the decay products of the working gas, and the molecular layering is thus mainly affected by the kinetics of decay of the molecules adsorbed onto the epitaxy surface. Evidently, the efficient development of such processes is hardly possible without detailed information on the kinetics of reactions on the substrate. Therefore, the

development of analytical methods suitable to determine the fragments concentration on the adsorbing surface is of extreme importance. Nowadays, sophisticated and expensive methods of electron diffraction and thermally programmed IR spectroscopy are used to accomplish this.

In this work, we demonstrate relatively simple methods to determine the surface concentrations of the working gas fragments and to elucidate the basic kinetic parameters of the processes occurring at the growth surface. The growth of silicon in a vacuum using hydride molecular sources is utilized as an example. The demonstrated approach was based on the kinetic simulation taking advantage of the experimental data on the silicon growth under conditions of an industrial process.

To the best of our knowledge, the papers published to date have been limited to the simplest kinetic models, accounting only for the hydride adsorption and for hydrogen desorption. This simplification is considered suitable to analyze the temperature dependence of the films growth rate. However, in the more general case, such simplified pyrolysis models (assuming complete decomposition of the hydride molecules at the stage of pre-chemisorption capture near the surface) contradict the experimental data on the composition of surface pyrolysis products. Moreover, the

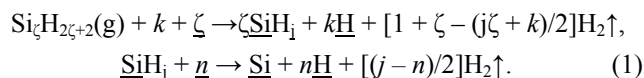
commonly used simplifications restrict the opportunities of the analysis of the processes on the silicon growth surface which determine the growing layer parameters (along with the growth rate).

Considering the monomolecular layer growth by molecular layering or the homo- and heteroepitaxy, the estimation of the decomposition products concentration by means of traditional kinetic analysis requires the knowledge on the rates of the absorbed fragments decomposition and the activation energy of the respective processes under the real technological conditions. Currently, the physicochemical and kinetic methods are intensively developed, extending the understanding of the processes at the substrate plate surface. Such models not only explain the observed effect of the absorbed fragments on the layer growth rate, but also forecast the behavior of complex systems under wide range of technological conditions. However, the models development is complicated by the ambiguity of the reaction mechanism, even in the cases of well established processes of monosilane and disilane decomposition. Due to this, the physicochemical models developed by different authors may be significantly different [1–4], and it is impossible to compare the absolute values of kinetic parameters, in particular, those of the chemisorption stage. The modern kinetic models of the epitaxial layers growth from the molecular beams accounting for the sequential stages of hydrides pyrolysis (chemisorption, interaction of the fragments at the surface, decomposition, and products desorption) have not been largely developed as well. Therefore, the description of the process characteristics basing on the general system of kinetic equations [5] and the estimation of the absorbed fragments concentrations are complicated if at all possible.

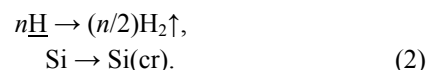
Rate equations of the hydrides molecules pyrolysis on the Si surface. In this work, by using the kinetic approximation and the available technological experimental data, we aimed at the elaboration of analytical equations suitable for calculation of the adsorbed fragments concentration on the crystal surface upon interaction of the latter with the molecular beam. These equations should also relate the rate of the adsorbed fragments decomposition with the other kinetic parameters. It was of evident importance to estimate how the derived kinetic parameters and their temperature dependences were affected by the choice of the pyrolysis model. The adsorption parameters were different in the cases of monosilane and disilane;

therefore, we compared the kinetics of their decomposition under conditions of silicon epitaxial growth. We considered the most commonly accepted models of $\text{Si}_\zeta\text{H}_{2\zeta+2}$ decomposition in the cases of monosilane ($\zeta = 1$) and disilane ($\zeta = 2$) with a single type of fragments present at the silicon surface, SiH_j . It was assumed that disilane molecule decomposed into two identical surface fragments, and the hydrogen atoms capture by the surface occurred via two different routes.

In general, monomolecular physicochemical processes on the silicon growth surface include capture of the gas molecule by the surface and the subsequent decomposition of the adsorbed molecule (either near the surface or on the growth surface). In the first stage, the molecules were adsorbed by Si surface with the formation of a SiH_j ($1 \leq j \leq 3$) fragment, whereas k of the detached hydrogen atoms, $0 \leq k \leq 2 + \zeta(2 - j)$, were captured by the free surface bonds. In the second stage the adsorbed SiH_j fragments decomposed; the so formed n hydrogen atoms ($0 \leq n \leq j$) were adsorbed by the n free surface bonds as well. The hydrogen atoms unbound to the surface were eliminated into the reactor volume. Therefore, the general scheme of the monomolecular reaction in the course of the pyrolysis at the silicon growth surface may be expressed as (1).



Besides the adsorption and pyrolysis stages, the processes of surface hydrogen H desorption and of the Si atoms incorporation into the growing crystal $\text{Si}(\text{cr})$ [Eq. (2)] were important in understanding the system behavior.



The reactions scheme and the corresponding set of the rate equations were somewhat complicated if several hydride fragment types were accounted for rather than a single one [6]. Below, the simplest pyrolysis scheme with a single type of surface fragments will be analyzed. The analysis of complicated systems with two or more of the fragments will be reported elsewhere.

The set of the rate equations (or the set of balance equations, under stationary conditions), corresponding to the scheme (1) was as follows:

$$\begin{aligned} \partial\theta_{\text{SiH}_j}/\partial t &= (k + \zeta)!(S_{\text{gas}}F_{\text{gas}}/n_s)(\theta_{\text{nbl}})^{k+\zeta} - \zeta(n+1)!v_{\text{SiH}_j}\theta_{\text{SiH}_j}(\theta_{\text{fr}})^n, \\ \partial\theta_{\text{H}}/\partial t &= k(k + \zeta)!(S_{\text{gas}}F_{\text{gas}}/n_s)(\theta_{\text{nbl}})^{k+\zeta} \\ &+ \zeta n(n+1)!v_{\text{SiH}_j}\theta_{\text{SiH}_j}(\theta_{\text{fr}})^n - m!\chi_{\text{H}}\theta_{\text{H}}^m, \end{aligned}$$

$$\begin{aligned}\partial\theta_{\text{fr}}/\partial t &= \zeta(n+1)!v_{\text{SiH}_3}\theta_{\text{SiH}_3}(\theta_{\text{fr}})^n - r_{\text{Si}}\theta_{\text{Si}}, \\ \theta_{\text{SiH}_3} + \theta_{\text{Si}} + \theta_{\text{H}} + \theta_{\text{fr}} &= 1, \\ \theta_{\text{fr}} &= \theta_{\text{bl}} + \theta_{\text{nbl}}.\end{aligned}\quad (3)$$

The surface concentrations n_x were related to the total number of the adsorption sites at the clean Si(100) surface, $n_s = 6.78 \times 10^{14} \text{ cm}^{-2}$. Therefore, $\theta_x = n_x/n_s$ were the dimensionless concentrations of the adsorbed hydride fragments (θ_{SiH_3}), silicon adatoms (θ_{Si}), hydrogen atoms (θ_{H}), and of the free surface bonds (θ_{fr}), respectively. The latter concentration included the bonds blocked with the fragments of the surface-captured molecules ($\theta_{\text{bl}} = j\theta_{\text{SiH}_3}$) and the non-blocked bonds ($\theta_{\text{nbl}} = \theta_{\text{fr}} - \theta_{\text{bl}}$). The factorial multipliers in Eq. (3) corresponded to the total number of the possible configuration of the adsorbed atoms and molecules on the two-dimensional surface lattice. The m index was 1 if single hydrogen atoms were desorbed from the surface and 2 in the case of their combination into hydrogen molecule during desorption. The rate constants v_{SiH_3} , χ_{H} , and r_{Si} , in Eq. (3) had the dimension of frequency (s^{-1}) and described the rates of adsorbed fragment decomposition, hydrogen desorption, and Si adatoms incorporation into the growing layer, respectively. The $S_{\text{gas}} = S(\text{SiH}_4)$ [or $= S(\text{Si}_2\text{H}_6)$] parameters corresponded to the adsorption ability of the silicon surface towards molecules of monosilane and disilane, respectively. The molecules flow $F_{\text{gas}} (\text{cm}^{-2} \text{ s}^{-1})$ was related to the gas pressure $P_{\text{gas}}(\text{Torr})$ in the reactor: $F_{\text{gas}} = 3.51 \times 10^{22} P_{\text{gas}} / (M_{\text{gas}} T_{\text{gas}})^{1/2}$, with T_{gas} being the gas temperature in the reactor ($^{\circ}\text{C}$) and M_{gas} being the molecular mass of the gas [7]. In the cases of the studied gases, therefore, $F(\text{SiH}_4) = 526.5 P(\text{SiH}_4)$ and $F(\text{Si}_2\text{H}_6) = 378.6 P(\text{Si}_2\text{H}_6)$. The surface concentration of silicon adatoms was related to the film growth rate $V_{\text{gr}}(\text{\AA}/\text{s})$ through the r_{Si} coefficient [Eq. (4)].

$$V_{\text{gr}} = l_0 r_{\text{Si}} \theta_{\text{Si}}. \quad (4)$$

For the calculations, the concentration of silicon atoms in the crystal volume was taken equal to $n_0 = 5.5 \times 10^{22} \text{ cm}^{-3}$; thus, $l_0 = (n_s/n_0) \times 10^{-8} = 1.23 \text{ \AA}$. The experimentally observed rate of silicon layer growth [8, 9] was the best fitted to the absolute temperature with Eq. (5).

$$\ln(V_{\text{gr}}) = V_2 + (V_1 - V_2) / \{1 + \exp[E_{\text{R}}/k_{\text{B}}T - C_{\text{R}}]\}. \quad (5)$$

In the case of monosilane: $V_1 = -1.1278 \text{ \AA}/\text{s}$, $V_2 = -6.28 \text{ \AA}/\text{s}$, $E_{\text{v}} = 1.1486 \text{ eV}$, and $C_{\text{R}} = 19.0317$ at the gas pressure in the reactor $P(\text{SiH}_4)$ of 0.3 mTorr [8]. In

the case of disilane: $V_1 = 0.976$ and $-1.51 \text{ \AA}/\text{s}$, $V_2 = -3.78$ and $-3.93 \text{ \AA}/\text{s}$, $E_{\text{v}} = 1.247$ and 1.736 eV , and $C_{\text{R}} = 19.146$ and 28.083 at $P(\text{Si}_2\text{H}_6)$ of 0.1 and of 0.01 mTorr, respectively [9].

The kinetic models reported in the literature [5, 10] to describe the temperature dependence of Si film growth rate accounted only for two processes: hydride adsorption and desorption of hydrogen. The first term, related to the working gas flow F_{gas} and the efficiency of its capture by the surface S_{gas} , determined the film growth rate at higher temperatures. The second term, determined by the surface saturation by hydrogen, limited the film growth at lower temperatures. The described approximation corresponded to $j = 0$, $n = 0$, and $k \neq 0$ in the Eqs. (1)–(3) set; in other words, it was assumed that the adsorbed molecules were completely decomposed into atoms in the first stage of pyrolysis, at the moment of the molecule capture by the growth surface. Then, if the number of non-blocked free bonds at the epitaxial surface was determined by the surface saturation with hydrogen, $\theta_{\text{nbl}} = \theta_{\text{fr}} = 1 - \theta_{\text{H}}$, the concentration of free surface bonds was unambiguously related to the film growth rate [Eq. (6)].

$$\begin{aligned}(k + \zeta)!(S_{\text{gas}}F_{\text{gas}}/n_s)(\theta_{\text{fr}})^{k+\zeta} &= V_{\text{gr}}/l_0, \\ k(k + \zeta)!(S_{\text{gas}}F_{\text{gas}}/n_s)(\theta_{\text{fr}})^{k+\zeta} &= m!\chi_{\text{H}}\theta_{\text{H}}^m.\end{aligned}\quad (6)$$

From the solution of Eq. (6), the silicon surface saturation with hydrogen can be obtained, and the film growth rate is related to the $S(\text{SiH}_4)$ and χ_{H} parameters. Redefining $\Phi = m!\chi_{\text{H}}/\{k(k + \zeta)!(S_{\text{gas}}F_{\text{gas}}/n_s)\}$, the second equation of the set Eq. (6) can be rewritten as Eq. (7).

$$(1 - \theta_{\text{H}})^{(k+\zeta)/m} = \Phi\theta_{\text{H}}. \quad (7)$$

In the case of hydrides pyrolysis at $(k + \zeta)/m = 2$, Eq. (7) can be further simplified.

$$1 - (2 + \Phi)\theta_{\text{H}} + \theta_{\text{H}}^2 = 0. \quad (8)$$

The analytical solution of Eq. (8), expressed in Eq. (9), allowed the relation of the concentration of free bonds at the epitaxial surface $\theta_{\text{fr}} = 1 - \theta_{\text{H}}$ to the film growth rate Eq. (10) and the expression of the film growth rate as a function of temperature, provided that the temperature behavior of hydrogen desorption coefficient is known.

$$\theta_{\text{H}} = (1 + \Phi/2) \pm [(1 + \Phi/2)^2 - 1]^{1/2}, \quad (9)$$

$$V_{\text{gr}} = (l_0 m! \chi_{\text{H}} / k) (1 - \theta_{\text{fr}})^m. \quad (10)$$

The latter mentioned coefficient was commonly expressed in the form of $\chi_{\text{H}} = \chi_0 \exp(-E_{\text{H}}^{\text{a}}/k_{\text{B}}T)$ with E_{H}^{a} ,

activation energy. The relation (10) was widely used in the literature to describe the experimental temperature behavior of the Si layer growth rate. The accuracy of Eq. (10) was, however, quite poor, and it could be directly applied only after introducing certain corrections, individual for each of the studied cases. Moreover, for reliable estimation using Eq. (10), the precise values of χ_H and S_{gas} over the whole range of the growth temperatures were required.

As was mentioned above, the simplified pyrolysis model did not allow the estimation of the fragments concentrations on the film surface in the course of the molecular layering. Noteworthy, according to the thermal desorption [10, 11] and IR spectroscopy [12] data, the presence of all probable fragments of silicon hydrides (SiH_j , $j = 1-3$) was possible at the lower range of the growth temperatures.

Below, we will describe the method to estimate the surface density of the adsorbed hydride fragments from the kinetic models and experimental data, and analyze the temperature behavior of an important but still poorly studied v_{SiH_j} parameter, determining the rate of the molecule decomposition on the adsorbing surface.

General solution of the rate equations set. The solution of the generalized problem of determining the surface concentrations of the decomposition products of the hydride molecular beam is based on the information on the constants included into the equations set (3) [13]. To date, the temperature behavior of the adsorption constant $S(\text{Si}_2\text{H}_6)$ [4, 14, 15] and of the hydrogen desorption constant χ_H [16–18] has been studied in detail. These constants determine the temperature dependence of the layer growth rate V_{gr} . Even though monosilane and disilane molecules were similar, the absolute values and the temperature dependences of their adsorption constants were significantly different. In particular, the disilane constant $S(\text{Si}_2\text{H}_6)$ was almost by an order of magnitude higher than that of monosilane, thus leading to the more efficient capture of disilane molecules by the surface. Hereinafter in the calculations we used $S(\text{SiH}_4) = 0.007$ [19]. The temperature dependence of $S(\text{Si}_2\text{H}_6)$ was discussed in [1–5]. At $300^\circ\text{C} < T_{\text{gr}} < 700^\circ\text{C}$, the $S(\text{Si}_2\text{H}_6)$ was accurately described by Eq. (11) with the negative activation energy [20].

$$S_{\text{Si}_2\text{H}_6}(T_{\text{gr}}) = 0.01458 + 2.0287\exp(-T_{\text{gr}}/148.83). \quad (11)$$

The coefficient corresponding to the silicon adatoms incorporation into the crystal lattice was

usually chosen high and independent of temperature ($r_{\text{Si}} \gg 1$), typical of the clean epitaxial silicon surface. Indeed, under assumption of the low and constant concentration of adatoms at the silicon surface, according to Eq. (4), $r_{\text{Si}} = r_0 V_{\text{gr}}(T_{\text{gr}})$, and r_0 depended solely on the working gas pressure and Si surface state. As $r_0 \sim \theta_{\text{Si}}$, and the adatoms concentrations under real conditions did not exceed 1%, the r_{Si} temperature dependence did not affect significantly the rate of molecules decomposition v_{SiH_j} .

The important parameter v_{SiH_j} , the rate of decomposition of the adsorbed hydride fragments $\text{Si}_\zeta\text{H}_{2\zeta+2}$, was poorly studied so far. To determine this parameter, we considered the general solution of the Eq. (3) set taking the following values as independent parameters.

$$\begin{aligned} \alpha &= V_{\text{gr}}/l_0, \\ \beta &= \theta_{\text{nbl}}^{(k+\zeta)} = \alpha/[(k+\zeta)!S_{\text{gas}}F_{\text{gas}}/n_s], \\ \gamma &= [1 - \beta^{1/(k+\zeta)} - \theta_H]. \end{aligned} \quad (12)$$

The parameters of Eq. (12) were expressed via the preset technological conditions (F_{gas} and T_{gr}) and the measured characteristics of the film growth (the rate of epitaxial silicon layers growth V_{gr} and the population density of Si surface with hydrogen θ_H). As the surface hydrogen was recognized as playing the important part in the hydride epitaxial processes, recently the above-mentioned parameters were studied in detail.

The analysis of the rate equations revealed that the knowledge of V_{gr} and θ_H was enough to reliably determine the surface concentrations of the decomposition products and to estimate the desorption characteristics of hydrogen atoms captured by the growth surface χ_H . By combining Eqs. (3) and (4), the relationship between those values could be easily derived; in the cases of monosilane and disilane molecules, the expression was reduced to a relatively simple form (13).

$$\chi_H = 1/(l_0 m!)(k+n)V_{\text{gr}}/\theta_H^m. \quad (13)$$

According to Eq. (13), the absolute value and the temperature dependence of χ_H under conditions of the layer growth could be determined by using the $V_{\text{gr}}(T_{\text{gr}})$, $\theta_H(T_{\text{gr}})$, both independently measurable in the technological experiment, in the theoretical model [8, 9].

By using the independent parameters Eq. (12) in the Eq. (3) set, the practically important surface concentration of the hydride fragments θ_{SiH_j} and the other surface concentrations could be easily calculated.

$$\begin{aligned}\theta_{\text{Si}} &= \alpha/r_{\text{Si}}, \\ \theta_{\text{SiH}_j} &= (\gamma - \theta_{\text{Si}})/(j + 1), \\ \theta_{\text{fr}} &= 1 - \theta_{\text{SiH}_j} - \theta_{\text{Si}} - \theta_{\text{H}}.\end{aligned}\quad (14)$$

Therefore, the fragments decomposition rate v_{SiH_j} on the silicon surface was related to the incorporation rate r_{Si} [Eq. (15)].

$$\begin{aligned}v_{\text{SiH}_j} &= \{j(1 + 1/j)^{n+1}/\zeta(n+1)!\} \alpha / \{(\gamma - \alpha/r_{\text{Si}})[\gamma \\ &+ (1 + 1/j)\beta^{1/(k+\zeta)} - \alpha/r_{\text{Si}}]^n\}.\end{aligned}\quad (15)$$

The dependence of the frequency of hydride fragments decomposition on the silicon layer growth rate was quite simple, and was determined in practice by the $(\gamma - \alpha/r_{\text{Si}})$ multiplier in Eq. (15). In order to determine the lower limit of the hydride decomposition rate on the silicon surface \tilde{v}_{SiH_j} (in the higher temperatures range, with r_{Si} being high, $\alpha/r_{\text{Si}} \ll 1$, $\gamma = (1 - \beta^{1/(k+\zeta)})$, and the surface saturation with hydrogen was close to zero), we expressed Eq. (15) in the form of Eq. (16).

$$\begin{aligned}\tilde{v}_{\text{SiH}_j} &= \{j(1 + 1/j)^{n+1}/\zeta(n+1)!\} \alpha / \{(1 - \beta^{1/(k+\zeta)})[1 - \beta^{1/(k+\zeta)} \\ &+ (1 + 1/j)\beta^{1/(k+\zeta)}]^n\}.\end{aligned}\quad (16)$$

The molecule decomposition rate depended solely on the highest layer growth rate, determined by the flow of the gas molecules to the surface. In the range of lower temperatures (at $V_{\text{gr}} > 0$) the conditions $\theta_{\text{H}} > 1$ and $\gamma \approx \beta^{1/(k+\zeta)}$ were held, therefore, and v_{SiH_j} should be estimated from Eq. (15).

Activation parameters of hydrogen desorption from Si surface. Analysis of the adsorbed hydrogen complexes, often determining the surface processes, is an important part of the vacuum hydride epitaxy studies. Due to widely used hydride epitaxy processes, the methods of hydrogen detection in the volume of crystalline silicon as well as on its surface have been intensively developed [5–10]. Hydrogen accumulated at the growth surface at low temperatures passivated the free bonds at the surface and at the defects of the crystal, thus improving some material properties. On the other hand, hydrogen adsorption significantly slowed down the films growth rate and thus limited the epitaxy applications to prepare hetero- and nano-compositions.

The hydrogen desorption coefficient was estimated by means of thermally regulated desorption spectroscopy [18, 21], however the scatter of the determined χ_{H} values was up to two orders of magnitude ($8 \times 10^{13 \pm 1} \text{ s}^{-1}$) [17, 22]. Such low

reproducibility was likely due to different experimental conditions. From the experimental $\chi_{\text{H}}(T)$ dependences derived by a variety of methods, the activation energy of hydrogen desorption from silicon surface E_{H}^a was 1.7–2.1 eV and did not vary much between the methods [22]. Evidently, for kinetic analysis the values of χ_{H} determined in the conditions close to the simulated ones should be used.

To simplify the calculations, the experimental $\theta_{\text{H}}(T)$ dependences [8, 9] were fitted with the Boltzmann functions [Eq. (17)].

$$\theta_{\text{H}}(T_{\text{gr}}) = \theta_2 + (\theta_1 - \theta_2) / \{1 + \exp[(T_{\text{gr}} - T_{\text{cr}})/\delta T]\}. \quad (17)$$

The fitting parameters were as follows: in the case of monosilane, $\theta_1 = 1.158$, $\theta_2 = -0.013$, $T_{\text{cr}} = 494.66$, and $\delta T = 46.35^\circ\text{C}$ at $P(\text{SiH}_4) = 0.3 \text{ mTorr}$ [8]; in the case of disilane, $\theta_1 = 0.997$ and 1.17 , $\theta_2 = 0.05435$ and -0.002 , $T_{\text{cr}} = 541.15$ and 454°C , and $\delta T = 59.182$ and 60.3°C at $P(\text{Si}_2\text{H}_6)$, of 0.1 and 0.01 mTorr , respectively [9]. The χ_{H} dependences of the reciprocal temperature as derived via Eq. (13) for the first-order ($m = 1$) and the second-order ($m = 2$) processes are shown in Fig. 1 in the cases of different pyrolysis models. The $\ln \chi_{\text{H}} = \ln \chi_0 - E_{\text{H}}^a/(k_{\text{B}}T)$ linear fitting gave the following activation energies E_{H}^a (eV): (a) 1.54 (1), 1.3 (2), 1.81 (3); (b) 2.0 (1), 2.09 (2), 2.75 (3). The slight deviation of the plots in Fig. 1 from the linear shape could be due to weak temperature dependence of the χ_0 multiplier as well as due to the inaccurately determined Si film growth rate at low temperatures and the saturation of Si surface with hydrogen at high temperatures. Indeed, at $T_{\text{gr}} < 500^\circ\text{C}$ the Si layer growth rate was below 1–2 Å/min, whereas at $T_{\text{gr}} > 650^\circ\text{C}$ the surface saturation with hydrogen was below 1%, thus accurate data could hardly be obtained. In spite of the mentioned sources of errors, the E_{H}^a values were close to those determined by the other methods [22]. The comparison of data in Fig. 1 with the other published results revealed that in the course of silicon growth from disilane source, the hydrogen desorption in the molecular form was the most probable, with the activation energy of $E_{\text{H}}^a \sim 1.9\text{--}2.1 \text{ eV}$. In the case of monosilane source, hydrogen was desorbed mainly in the atomic form, with $E_{\text{H}}^a \sim 1.9 \text{ eV}$.

The temperature behavior and absolute value of hydrides decomposition on the growth surface was not much discussed in the literature, to the best of our knowledge. In the estimations, the Arrhenius form of the temperature dependence was commonly accepted, with the activation energy derived from the model

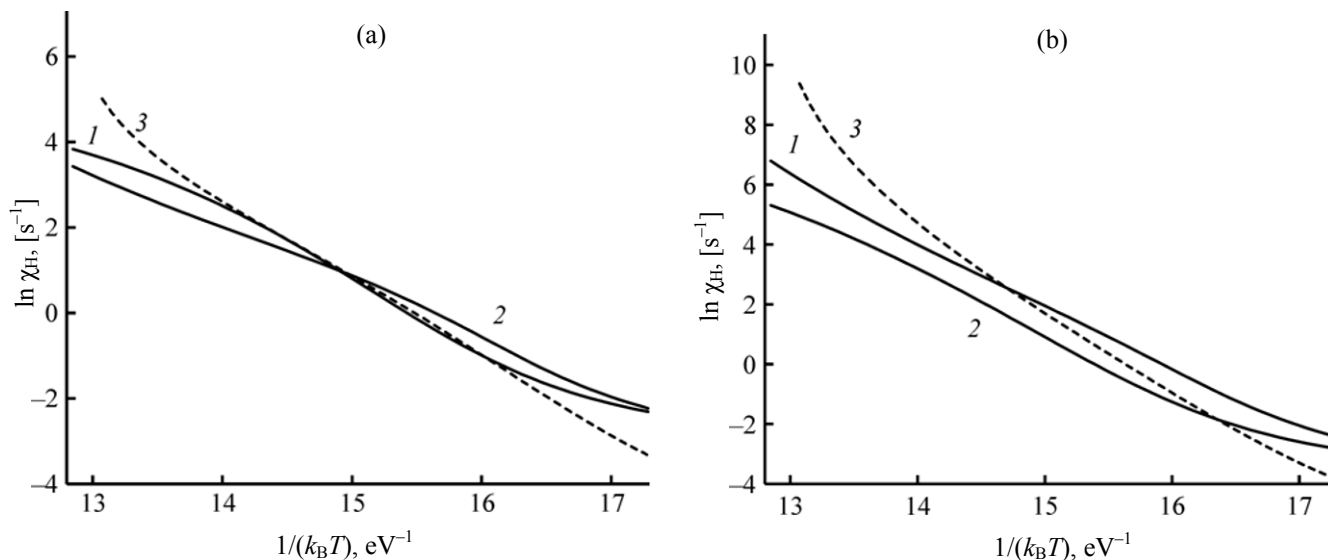


Fig. 1. The constant of hydrogen desorption from silicon surface χ_H as a function of temperature under conditions of Si film growth from disilane at (1) $P(\text{Si}_2\text{H}_6) = 0.1$ and (2) 0.01 mTorr [9] and from monosilane at (3) $P(\text{SiH}_4) = 0.3$ mTorr [8]; model: $(jkn) = (303)$ with (a) $m = 1$ and (b) $m = 2$.

calculations [23]. However, the purely Arrhenius dependence of the surface molecules decomposition over the whole growth temperature range ($400\text{--}700^\circ\text{C}$) was unlikely, as the interaction of the adsorbed molecules with the free ($T_{\text{gr}} > 650^\circ\text{C}$) and hydrogen-filled ($T_{\text{gr}} < 550^\circ\text{C}$) surface should occur via different mechanisms.

The rate parameters of the adsorbed molecules pyrolysis could be determined via dynamic IR spectrometry. However, using this method under real technological conditions was very complicated, as the weak signal of the adsorbed molecules at the mid-IR and far-IR oscillation-rotational frequencies should be detected [3, 24].

In this work, the parameter v_{SiH_j} was studied in the frame of the kinetic model using the indirect experimental data from the referenced literature. The calculations performed gave important information on the lifetime of the pyrolysis products on the growth surface and allowed elucidation of the surface reaction mechanisms as well as the type of the adsorbed molecules interaction with the film surface.

By using Eq. (15), the temperature behavior of the decomposition rate of the silanes was analyzed under certain conditions of the growth experiment. The calculated curves corresponding to the most commonly accepted pyrolysis models are given in Figs. 2 and 3.

The technological process parameters were taken from [8, 9]; the experimental temperature functions of the film growth rate and the surface saturation with hydrogen was accurately described by Eqs. (5) and (17). The commonly accepted value of 0.007 was chosen for the adsorption ability for monosilane $S(\text{SiH}_4)$ 0.007. The adsorption ability for disilane was much higher and changed monotonously from 0.2 to 0.03 at $400\text{--}700^\circ\text{C}$ according to Eq. (11).

The curves in Fig. 2a revealed the unusual dependence of the pyrolysis rate on the growth temperature as well as the strong dependence of it on the reactor pressure. The shown curves corresponded to the most commonly applied model assuming the domination of the SiH_3 on the surface and transition of all hydrogen atoms from hydride onto the growth surface. Figure 2b shows the corresponding curves in the case of disilane under assumption of the fragment SiH dominating on the growth surface. The comparison of the curves in Fig. 2 revealed that the decrease in the disilane pressure in the chamber significantly decreased the molecules pyrolysis on the growth surface. Similar curves for other models of monosilane and disilane decomposition are presented in Fig. 3.

The frequency dependences of hydride pyrolysis on the growth temperature (Figs. 2 and 3) were quite

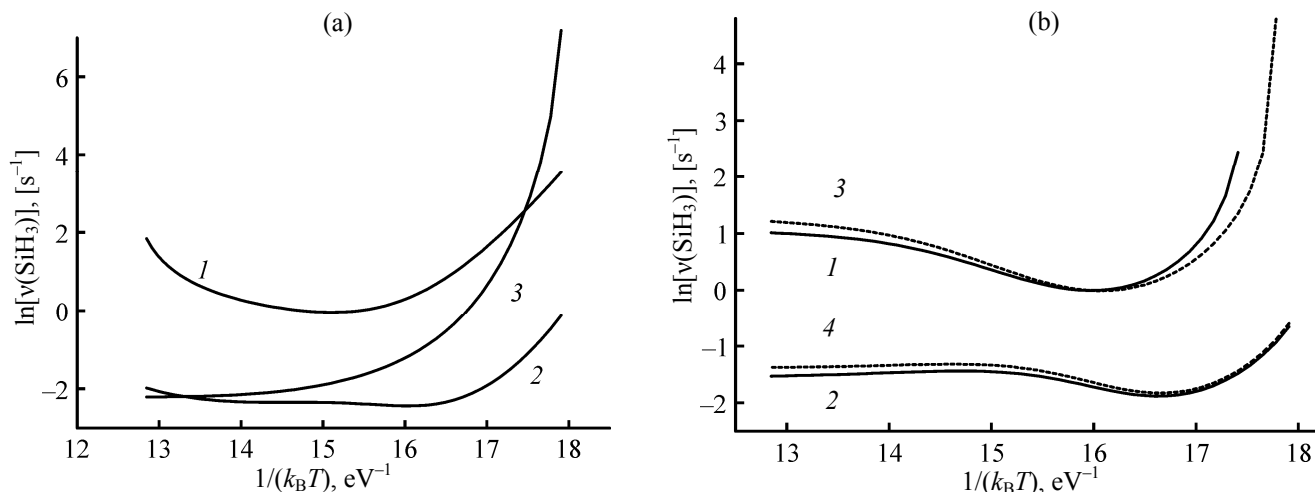


Fig. 2. Hydrides pyrolysis frequency on the Si growth surface as a function of temperature, at $r_{\text{Si}} = 100V_{\text{gr}}$. Models: (a) $P(\text{Si}_2\text{H}_6)$ 0.1 mTorr, $(jkn) = (303)$ (1); $P(\text{Si}_2\text{H}_6)$ 0.01 mTorr, $(jkn) = (303)$ (2); $P(\text{SiH}_4)$ 0.3 mTorr, $(jkn) = (313)$ (3); (b) $P(\text{Si}_2\text{H}_6)$ 0.1 mTorr, $(jkn) = (141)$ (1); $P(\text{Si}_2\text{H}_6)$ 0.01 mTorr, $(jkn) = (141)$ (2); $P(\text{Si}_2\text{H}_6)$ 0.1 mTorr, $(jkn) = (121)$ (3); $P(\text{Si}_2\text{H}_6)$ 0.01 mTorr, $(jkn) = (121)$ (4).

complex and could be described by the Arrhenius function with a single activation energy only at $T_{\text{gr}} > 600^\circ\text{C}$ corresponding to the pyrolysis at the relatively clean surface, free of the adsorbed hydrogen. The curves shown in the figures were obtained in the frame of models corresponding to the capture of the SiH_j fragments with different mechanisms of hydrogen transfer from the hydride molecule to the surface. The most prominent difference in the high-temperature decomposition behavior was observed in the models assuming that the hydrogen transfer to the surface and its capture by the surface occurred at different stages of the molecule pyrolysis. In particular, in the case of the (303) model of disilane pyrolysis (Fig. 2a) the hydrogen atoms were transferred to the surface from the SiH_3 adsorbed by the silicon specimen, whereas in the case of (141) model (Fig. 2b) the hydrogen atoms were mainly adsorbed on the surface from the prechemisorption state ($k = 4$) and only a single atom ($n = 1$) was transferred to the surface from the captured SiH fragment. Similar features are characteristic of the other silane pyrolysis schemes, as demonstrated by different shape of the curves in Figs. 2 and 3. If the hydrogen atoms were mainly transferred to the surface in a single stage, the type of the temperature dependence of the pyrolysis rate was weakly affected by the number of the transferred hydrogen atoms desorbing to the reactor volume and on the type of the SiH_j ($j = 1\text{--}3$) fragment prevailing on the adsorbing surface.

Further analysis of the curves in Figs. 2 and 3 demonstrated that the temperature dependence of v_{SiH_j} in the studied temperature range was affected by the choice of the pyrolysis model. In the high-temperature range, the $v_{\text{SiH}_j}(T)$ data fitting with the Arrhenius function $v_{\text{SiH}_j}(T) = v_0 \exp(-E_a/k_B T)$ gave the activation energy $E_a \sim 0.00\text{--}0.14$ eV in the case of monosilane decomposition. The activation energy of disilane pyrolysis was of $0.2\text{--}1.5$ eV at $P(\text{Si}_2\text{H}_6) = 0.1$ mTorr depending on the pyrolysis model. With decreasing gas pressure, the activation energy was reduced to the value close to that in the case of monosilane (Fig. 2).

At lower growth temperature the shape of the pyrolysis frequency dependence was determined by the hydrogen capture on the surface from the adsorbed hydride fragment (Fig. 3). In the cases of all dependences presented in Fig. 3 the number of hydrogen atoms adsorbed on the growth surface from the molecule was the same ($k + n = 2$). However, in the cases of the models with different (jkn) , the mechanism of the hydrogen capture by the surface could be substantially different. This was reflected in the activation energy values. In the case of monosilane, at $k > 1$ and $n = 0$ the pyrolysis activation energy was $\sim 0.12\text{--}0.14$ eV, whereas at $k = 0$ and $n > 1$, $E_a \sim 0.08$ eV. In the case of disilane, on the contrary, at $k > 1$ and $n = 0$, $E_a \sim 0.12\text{--}0.6$ eV, whereas at $k = 0$ and $n > 1$, $E_a \sim 1.0\text{--}1.5$ eV. If hydrogen was completely transferred from the molecule to the surface, then in

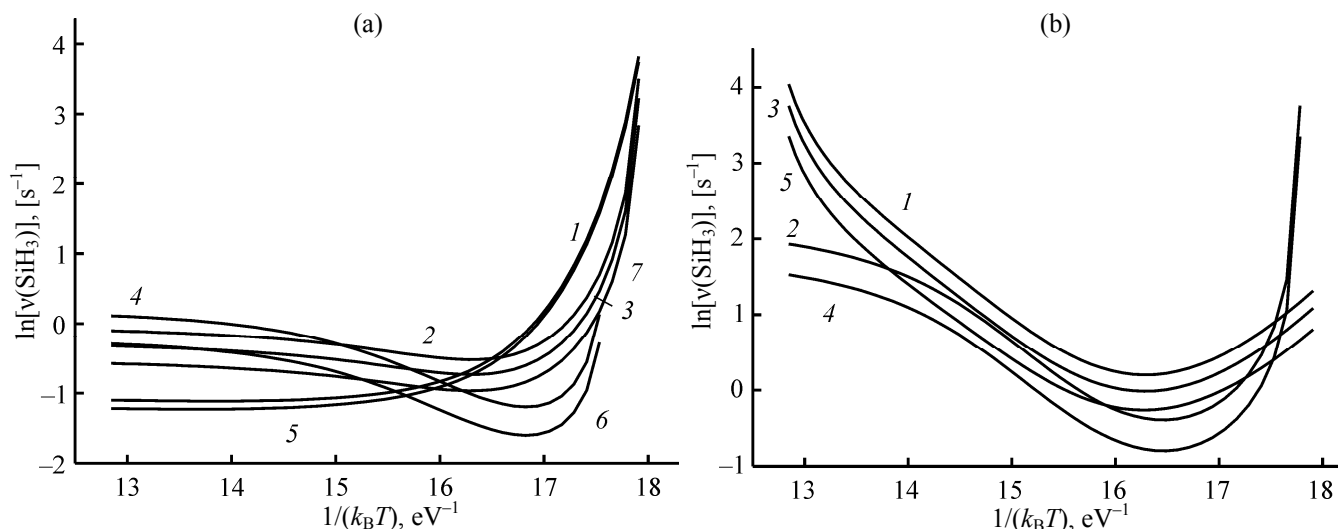


Fig. 3. Pyrolysis frequency of monosilane at (a) $P(\text{SiH}_4)$ 0.3 mTorr and (b) disilane at $P(\text{Si}_2\text{H}_6)$ 0.1 mTorr on the Si growth surface as a function of temperature, at $r_{\text{Si}} = 100V_{\text{gr}}$ and $k + n = 2$. Models (jkn): (a) (302) (1), (311) (2), (211) (3), (220) (4), (202) (5), (120) (6), (111) (7); (b) (301) (1), (220) (2), (201) (3), (120) (4), (101) (5).

the case of monosilane $E_a \sim -0.07$, -0.009 , and 0.05 eV for the (313), (222), and (131) models, respectively, and in the case of disilane, $E_a \sim 1.05$, 0.077 , and 0.2 eV for the (303), (222), and (141) models, respectively.

At low growth temperature, in the cases of all models used, the pyrolysis frequency dependences were not described by the activation energy; moreover, the hydride decomposition was accelerated upon cooling, as previously described in the studies of monosilane [25] and disilane [26]. In the case of disilane at high temperature ($T_{\text{gr}} = 700^\circ\text{C}$) v_{SiH_j} was ranged from 57 s^{-1} [(301) model] to 4.6 s^{-1} [(120) model]. After cooling to $T_{\text{gr}} = 480^\circ\text{C}$ the pyrolysis frequency range was 0.45 s^{-1} [(120) model] to 1.3 s^{-1} [(301) model]. In the case of monosilane the same parameter ranged from 0.3 s^{-1} [(202) model] to 1.1 s^{-1} [(220) model] at $T_{\text{gr}} = 700^\circ\text{C}$, and from 0.24 s^{-1} [(120) model] to 2 s^{-1} [(302) model] at $T_{\text{gr}} = 450^\circ\text{C}$.

The decrease of hydrogen surface concentration with decreasing the gas pressure in the chamber led to increase of the free surface sites concentration and to a higher content of the adsorbed molecular fragments. As seen from the curves in Figs. 2 and 3, this in turn led to slowing down of the surface decomposition of the molecules, to decrease in the silicon adatoms concentration on the surface, and thus to deceleration of the film growth. Noteworthy, the shape of the curves was sensitive to the temperature behavior of the surface saturation with hydrogen, whereas the effect of

other parameters was weaker. As demonstrated in Fig. 4, even slight change in the $\theta_{\text{H}}(T_{\text{gr}})$ dependence could significantly change the $v(\text{SiH}_2)(T_{\text{gr}})$ shape. The analysis of the data gave clearer insight into the nature of the unusual (non-Arrhenius) temperature behavior of v_{SiH_j} .

In particular, Fig. 4 shows the temperature behavior of v_{SiH_j} derived by using the $\theta(T_{\text{gr}})$ fitting equation (17) with varied parameters. From the shape of the curves it followed that the model based on different mechanisms of the pyrolysis under conditions of the low and high Si surface saturation with hydrogen gave the result closest to the experimental one. In the frame of this model, the temperature behavior of the hydride decomposition rate was described by a sum of two activation dependences with E_{a1} and E_{a2} , corresponding to the decomposition on the clean (high temperature) and hydrogen-covered (low temperature) silicon surface [Eq. (18)].

$$v_{\text{SiH}_j} = v_{01}(1 - \theta_{\text{H}})\exp[-E_{a1}/(k_{\text{B}}T)] + v_{02}(\theta_{\text{H}})\exp[-E_{a2}/(k_{\text{B}}T)]. \quad (18)$$

The pre-exponential factors $v_{01(2)}(\theta_{\text{H}})$ in Eq. (18) depend on the of the surface with hydrogen, and, therefore, on the growth temperature. In the simplest case, $v_{01}(1 - \theta_{\text{H}})$ could be considered constant, and $v_{02}(\theta_{\text{H}})$ was linear with the surface saturation with hydrogen. Then, according to Eq. (17), $v_{02}(\theta_{\text{H}})$ could be expressed as Eq. (19), similar to the θ_{H} temperature

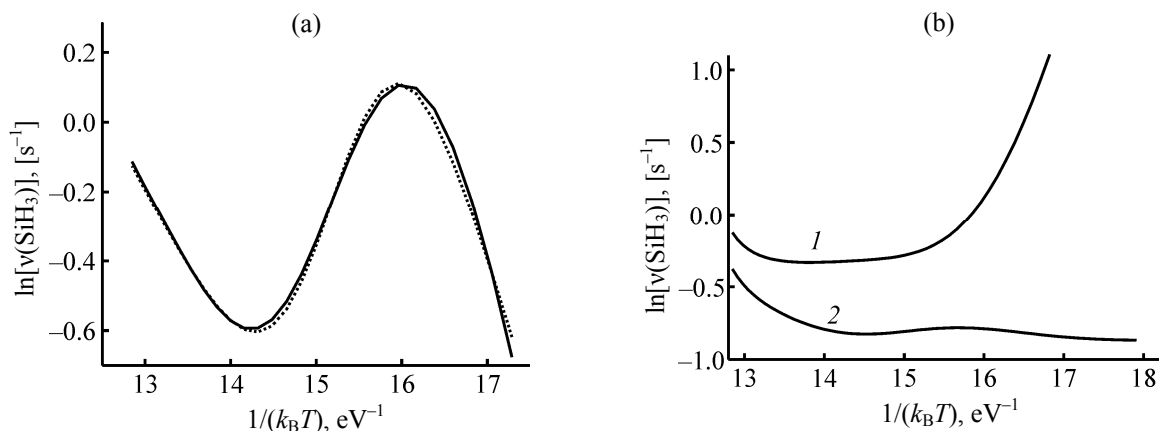


Fig. 4. Pyrolysis frequency of disilane on the Si growth surface as a function of reciprocal temperature. Solid lines computed at $r_{\text{Si}} \gg 1$ and $(jkn) = (303)$. The $\theta_{\text{H}}(T_{\text{gr}})$ function is fitted with Eq. (17) at: (a) θ_1 0.742, θ_2 0.149, T_{cr} 560.12°C, δT 33.25°C; (b) θ_1 0.943, θ_2 0.05435, T_{cr} 541.15°C, δT 59.182°C (1); θ_1 0.643, θ_2 0.05435, T_{cr} 560°C, δT 38°C (2). (Dashed lines) correspond to modeling with Eqs. (18) and (19) at v_{01} 352 s⁻¹, E_{a1} 0.47 eV, v_{02} 5.95 × 10⁶ s⁻¹, E_{a2} 0.95 eV, T_{cr} 517°C, δT 19.5°C.

behavior. The corresponding dependence is shown in Fig. 4a by a dashed line.

$$v_{02}\theta_{\text{H}} = v_{02}F(T_{\text{gr}}) = v_{02}/\{1 + \exp[(T_{\text{gr}} - T_{\text{cr}})/\delta T]\}. \quad (19)$$

The observed non-monotonic temperature dependences could be explained as follows. At higher growth temperatures, 600–700°C, the molecule was decomposed via cleavage of hydrogen atom and its capture by the free surface bond. In the case of disilane, the activation energy (averaged along all the pyrolysis models) was relatively high, $E_a \sim 0.78$ eV; monosilane pyrolysis possessed an order of magnitude lower activation energy, $E_a \sim 0.052$ eV. Noteworthy, the E_a values varied a lot depending on the model: in the case of disilane, from 0.08 eV [(222) model] to 1.5 eV [(301) model]; in the case of monosilane, from –0.08 eV [(303) model] to 0.14 eV [(301) model]. In both cases, the lower activation energies corresponded to $k > n$ processes, the hydrogen capture by the surface mainly in the stage of pre-chemisorption capture of the decomposing molecule. The higher activation energies corresponded to $k < n$ processes, the hydrogen capture by the surface mainly from the adsorbed molecule. The lower activation energy values, typical of monosilane decomposition at higher temperatures, were consistent with the molecular theory [2, 4]. In these works, lower potential barrier was derived in the case of monosilane sorption as compared to disilane. That finding contradicted the opposite relation of the capture coefficient, commonly explained by the bond energy difference: Si–H (3.9 eV) in monosilane and Si–Si (3.3 eV) in disilane. The revealed contradiction indicated likely that adsorption and surface pyrolysis

of the hydride molecules occurred via different mechanisms even at higher temperatures, on the hydrogen-free surface. The surface-captured disilane fragments decomposed with the Si–H bond cleavage and the subsequent hydrogen atoms adsorption. The adsorbed monosilane fragments likely decomposed via hydrogen atoms transfer from the molecule onto the free surface bonds via the intermediate excited states as suggested in [23].

At lower growth temperature (450–550°C) the free surface bonds of silicon were efficiently populated by hydrogen atoms. This increased the energy required to decompose the surface hydride fragment. For example, hydrogen atoms of SiH_j and adsorbed hydrogen atoms could recombine into hydrogen molecule to facilitate hydrogen desorption. The difference in the mechanism of hydrogen atoms transfer from the hydride molecule to the surface, either involving surface-adsorbed hydrogen or not, could be the factor leading to the difference in the observed activation energy. As the pyrolysis involving surface hydrogen occurred at lower temperatures, this mechanism might not be revealed explicitly in the plots. However, at the intermediate growth temperatures (450–600°C) the surface hydrogen concentration was sharply increased upon cooling, and the pyrolysis involving adsorbed hydrogen led to the accelerated hydride molecule decomposition with decreasing growth temperature. Thus, the observed unusual dependence of v_{SiH_j} on the growth temperature was due to the change in the mechanism of surface decomposition of hydride.

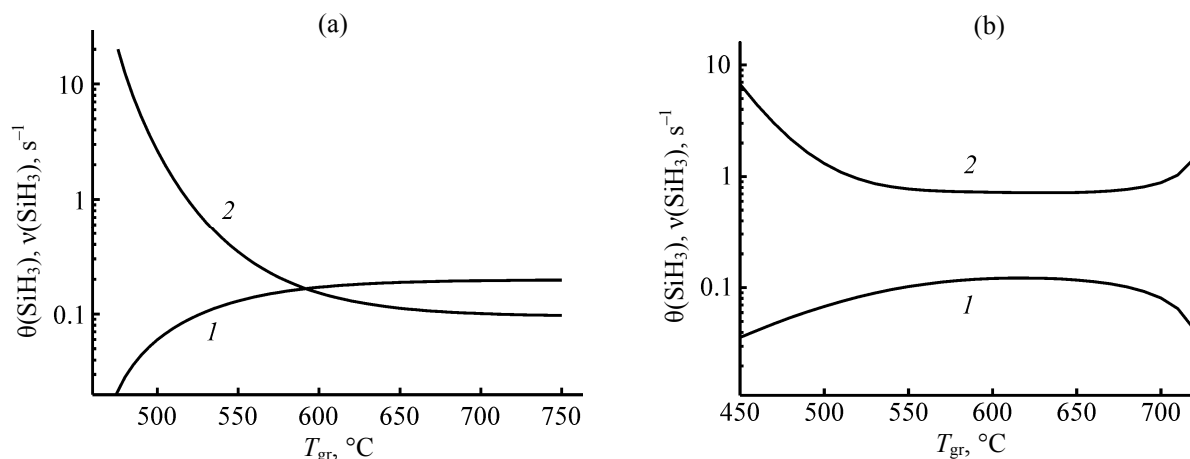


Fig. 5. Surface concentration of the fragments $\theta(\text{SiH}_3)$ (1) and the molecule decomposition rate (2) as functions of temperature, in the cases of monosilane (a) and disilane (b) at $P(\text{SiH}_4)$ 0.3 mTorr and $P(\text{Si}_2\text{H}_6)$ 0.1 mTorr, model $(jkn) = (303)$.

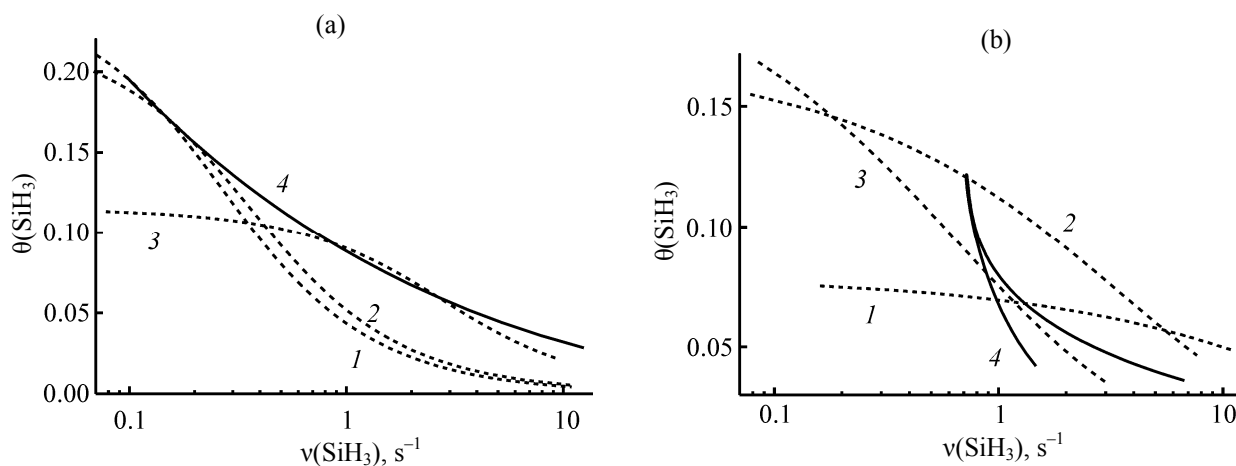


Fig. 6. Surface concentration of the fragments $\theta(\text{SiH}_3)$ as a function of monosilane (a) and disilane (b) decomposition rate at T_{gr} : 700°C (1), 600°C (2), 500°C (3), and under conditions (4). Curves 1–3: pyrolysis rate is changed with the growth rate via non-thermal activation of decomposition.

In addition to the surface reactions rate, the kinetic analysis allowed the determination of the surface concentrations of the components under different conditions. In the case of hydrides pyrolysis on the silicon growth surface, the surface concentration of the decomposing fragments (SiH_3) and the number of unoccupied bonds were given by relations (14); taking into account the dependence of layer growth rate on temperature, we could as well predict temperature behavior of the variables from equations (14) (Figs. 5a, 5b, curves 1). The curves 2 in the same figures show the temperature dependence of SiH_3 decomposition rate as derived in the case of $(jkn) = (303)$ silanes pyrolysis model. The dependence of surface concentration of hydride fragments on their decom-

position rate [according to Eqs. (14) and (15)] was somewhat more complex (Figs. 6a, 6b, curves 4). Our calculations revealed the differences between temperature behavior of the surface concentration $\theta(\text{SiH}_2)$ as well as of the pyrolysis rate $v(\text{SiH}_2)$ depending on the silane nature. In particular, in the case of monosilane, with heating $\theta(\text{SiH}_2)$ increased monotonously, and $v(\text{SiH}_2)$ decreased, whereas in the case of disilane the curves shape was different, pointing at the possible change in the mechanism of hydrogen transfer to the growth surface.

Even though in the case of any certain model the pyrolysis rate $v(\text{SiH}_2)(T_{\text{gr}})$ was unambiguously determined by Eq. (15), in general, it could change at

the fixed temperature if the molecules decomposition was excited by the resonance high-frequency irradiation [12, 24]. In this case, even at low temperatures the layer growth could be significantly accelerated [26, 27]. The dependences of Si surface saturation degree with SiH₃ on the decomposition rate $v(\text{SiH}_2)$ are shown in Figs. 5a, 5b (curves 1–3 for different growth temperatures). In the frame of the $(jkn) = (303)$ model, at $550^\circ\text{C} < T_{\text{gr}} < 650^\circ\text{C}$, $v(\text{SiH}_2)$ was ranged from 0.1 to 0.35 s⁻¹ (monosilane) and from 0.07 to 0.08 s⁻¹ (disilane). The increase in $v(\text{SiH}_2)$ at given temperature expectedly led to lower surface saturation with the decomposing fragments due to the layer growth acceleration.

ACKNOWLEDGMENTS

This work was financially supported by the Federal Target Program “Scientific and Pedagogical Personnel of Innovative Russia 2009–2013” (projects 2012-1.2.1-12-000-2013-095 and 2011-1.3.2-200-023-030).

REFERENCES

- Shi, J., Tok, E.S., and Kang, H.C., *J. Chem. Phys.*, 2007, vol. 127, p. 164713.
- Ng, R.Q.M., Tok, E.S., and Kang, H.C., *J. Chem. Phys.*, 2009, vol. 131, p. 044707.
- Shinohara, M., Seyama, A., Kimura, Y., and Niwano, M., *Phys. Rev. (B)*, 2002, vol. 65, p. 075319.
- Smardon, R.D. and Srivastava, G.P., *J. Chem. Phys.*, 2005, vol. 123, p. 174703.
- Taylor, N., Kim, H., Desjardins, P., Foo, Y.L., and Greene, J.E., *Appl. Phys. Lett.*, 2000, vol. 76, p. 2853.
- Potapov, A.V. and Orlov, L.K., *Phys. Stat. Solidi (C)*, 2003, vol. 195, no. 3, p. 853.
- Grave, D.V., *Mater. Sci. Eng. B*, 1993, vol. 18, p. 22.
- Kim, K.J., Suemitsu, M., Yamanaka, M., and Miyamoto, N., *Appl. Phys. Lett.*, 1993, vol. 62, p. 3461.
- Murata, T., Nakazawa, H., Tsukidate, Y., and Suemitsu, M., *Appl. Phys. Lett.*, 2001, vol. 79, p. 746.
- Gates, S.M., Greenlief, C.M., and Beach, D.B., *J. Chem. Phys.*, 1990, vol. 93, p. 7493.
- Wright, S. and Hasselbrink, E., *J. Phys. Chem.*, 2001, vol. 114, p. 7228.
- Shinohara, M., Seyama, A., Kimura, Y., and Niwano, M., *Phys. Rev. (B)*, 2002, vol. 65, p. 075319.
- Tovbin, Yu.K., *Teoriya fiziko-khimicheskikh protsessov na granitse gaz-tverdoe telo* (Theory of Physico-chemical Processes at the Gas-Solid Interface), Moscow: Nauka, 1990.
- Kang, J.K. and Musgrave, C.B., *Phys. Rev. (B)*, 2001, vol. 64, p. 245330.
- Gates, S.M. and Kulkarni, S.K., *Appl. Phys. Lett.*, 1991, vol. 58, p. 2963.
- Sinniah, K., Sherman, M.G., Lewis, L.B., Weinberg, W.H., Yates, J.T., and Janda, K.C., *Phys. Rev. Lett.*, 1989, vol. 62, no. 5, p. 567.
- Greenlief, C.M. and Lier, M., *Appl. Phys. Lett.*, 1994, vol. 64, no. 5, p. 601.
- Price, R.W., Tok, E.S., and Zhang, J., *J. Crystal Growth*, 2000, vol. 209, nos. 2–3, p. 306.
- Potapov, A.V., Orlov, L.K., and Ivin, S.V., *Thin Solid Films*, 1999, vol. 336, p. 191.
- Ferguson, B.A., Reeves, C.T., Safarik, D.J., and Mullins, C.B., *J. Phys. Chem.*, 2000, vol. 113, p. 2470.
- Hofer, U., Li, L., and Heinz, T.F., *Phys. Rev. (B)*, 1992, vol. 45, p. 9485.
- Orlov, L.K. and Smyslova, T.N., *Semiconductors*, 2005, vol. 39, no. 11, p. 1275.
- Vittadini, A. and Selloni, A., *Phys. Rev. Lett.*, 1995, vol. 75, no. 26, p. 4756.
- Pauleau, Y. and Tonneau, D., *J. Appl. Phys.*, 2002, vol. 91, no. 3, p. 1553.
- Orlov, L.K., Ivin, S.V., and Smyslova, T.N., *Russ. J. Phys. Chem. B*, 2011, vol. 5, no. 1, p. 168.
- Orlov, L.K. and Smyslova, T.N., *Tech. Phys.*, 2012, vol. 82, no. 11, p. 1547.
- Orlov, L.K. and Ivin, S.V., *Semiconductors*, 2011, vol. 45, no. 4, p. 557.